Optical and Quantum Electronics (2019) 51:156
https://doi.org/10.1007/s11082-019-1867-z

Topological plasmonic modes in graphene-coated nanowire arrays

Peng Meng[1] · Dong Zhao[1] · Dong Zhong[1] · Weiwei Liu[2]

Received: 15 November 2018 / Accepted: 23 April 2019
© Springer Science+Business Media, LLC, part of Springer Nature 2019

Abstract
We investigate the topological edge modes of surface plasmonic polaritons (SPPs) in a two-dimensional waveguide array composed of graphene-coated nanowires. The system experiences topological phase transition by tuning the inter-layer spacing between adjacent unit cells. The topological modes emerge at the edge of topological non-trivial nanowire arrays when the intra-layer spacing is larger than the inter-layer spacing. Thanks to the strong confinement of graphene SPPs, the modal wavelength of topological edge modes can be squeezed as small as 1/20 of incident wavelength. The study provides a promising approach to realizing robust light transport beyond diffraction limit.

Keywords Graphene waveguides · SPPs · Topological edge modes

1 Introduction

Surface plasmon polaritons (SPPs), supported at the interface of metal and dielectric, have attracted much attention as they can conquer diffraction limit and realize strong local field enhancement (Kou et al. 2013; Wang et al. 2017a; Sun et al. 2016; Kou and Förstner 2016; Huang et al. 2017; Peng et al. 2017; Liu et al. 2016, 2018a; Chen et al. 2018). Recently, graphene, a two-dimensional material composed of carbon atoms, has been reported to support SPPs in the infrared and terahertz frequencies (Bao and Loh 2012; Deng et al. 2015a, b, 2016a; Zhao et al. 2018; Ke et al. 2018a; Li et al. 2012; Lin et al. 2016a, b; Ke et al. 2016, 2017a, 2018a, b; Liu et al. 2018b; Zhang et al. 2014). The SPPs in graphene manifest many new features when compared with that in metal, such as the strong field confinement, the flexible tunability via electrostatic and chemical doping, the broadband

Peng Meng and Dong Zhao have contributed equally to this work.

✉ Dong Zhong
27820424@qq.com

✉ Weiwei Liu
lwhust@hust.edu.cn

[1] School of Electronics and Information Engineering, Hubei University of Science and Technology, Xianning 437100, China

[2] School of Physics, Huazhong University of Science and Technology, Wuhan 430074, China

optical response, the strong nonlinear effect, and the high carrier mobility (Bao and Loh 2012; Ke et al. 2017a; Deng et al. 2015a; Wang et al. 2017b; Zhao et al. 2017; Hong et al. 2017, 2018; Li et al. 2019a, b; Liu et al. 2019; He et al. 2019; Ni et al. 2016). Multiple coupled graphene waveguides, graphene sheets arrays, and graphene metamaterials are proposed to manipulate the optical property and the propagation of SPPs (Ke et al. 2018b, c; Zhang et al. 2014; Zhao et al. 2019).

On the other hand, topological photonics have also attracted enormous interest in recent years (Lu et al. 2014; Deng et al. 2018; Wang et al. 2017c, 2018; Liu and Wakabayashi 2017; Qin et al. 2018). Topological band theory characterizes the collective behavior of the wave functions on the energy band, which provides new possibility to reveal new states of light (Lu et al. 2014). One prominent feature of topological theory is that topological protected bound states appear at the interface of two topological distinct media. The bound modes are robust against the structure disorder (Deng et al. 2016b; Ge et al. 2017). A simple model to understand the topological phenomenon is the so called Su–Schrieffer–Heeger (SSH) model, which consists of binary periodic arrays (Ge et al. 2015; Blanco-Redondo et al. 2016; Pocock et al. 2018; Ke et al. 2017b; Ke et al. 2019). The arrays possess two different topological phases according to the ratio of inter-layer coupling to intra-layer coupling. Topological bound modes appear when the two structures with different topological phases are interfaced. The topological bound modes based on SSH model are theatrically and experimentally demonstrated in plasmonic systems, including metallic waveguides (Cheng et al. 2015), graphene sheets (Ge et al. 2015), and metallic nanoparticles (Pocock et al. 2018). Most of the studies are focused on one-dimensional arrays.

In this work, we investigate a two-dimensional extension of the SSH model, that is, the topological plasmonic modes in a graphene-coated nanowire array with the square lattice. The band structure and field distributions of Bloch mode for the periodic arrays are studied. We show the band inversion and the topological phase transition take place when the inter-layer spacing is equal to intra-layer spacing. The topological edge modes in the finite waveguide arrays are also discussed in details.

2 Geometry

Figure 1 depicts the geometric diagram of graphene-coated nanowire array. The array is periodic along x and y direction and placed in a square lattice. The SPPs propagate along z direction. Each unit cell consists of four nanowires with the radius denoted as a. The intra-layer spacing in each unit cell along x and y direction is uniform, which is labeled as d_1. The inter-layer spacing between different unit cells is d_2. The nanowires are embedded in the host dielectric medium with the relative permittivity denoted by ε_b. Here we consider the dielectric is air with $\varepsilon_d = 1$ for simplicity. The dielectric core is assumed to be silicon dioxide. The relative permittivity of SiO_2 is given by $\varepsilon_d = 3.9$. The surface conductivity of graphene σ_g can be modeled by the Kubo formula (Bao and Loh 2012), which relates to the temperature T, chemical potential μ_c, relaxation time τ, and incident wavelength λ. In this work, the room temperature ($T = 300$ K) is assumed. The chemical potential, relaxation time and incident wavelength are $\mu_c = 0.5$ eV, $\tau = 0.5$ ps, and $\lambda = 12$ μm, respectively. Then, the surface conductivity of graphene is figured out as $\sigma_g = 4.83 \times 10^{-6} + 3.71i \times 10^{-4}$ S. Since the real part of surface conductivity is very small as compared to its imaginary part, the influence of intrinsic loss of graphene is found to be negligible.

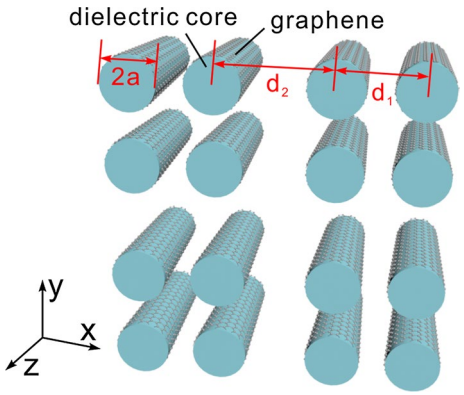

Fig. 1 Schematic of a two-dimensional array of dielectric nanowires coated by graphene monolayer

Numerical simulations are performed with the commercial software COMSOL Multiphysics based on finite element method. The graphene is modeled by using the surface current boundary condition (Huang et al. 2017). Only single unit cell is needed in the simulation. The periodic boundary condition is utilized in the x and y directions. The domain has been discretized by using an inhomogeneous mesh with the maximal element size being $<1/12$ of the wavelength of SPPs. The effective refractive index and field distributions of eigenmode can be obtained using mode analysis. The two dimensional dielectric nanowire arrays can be firstly fabricated by lithographic techniques. Then the graphene can be coated to nanowire templates by chemical-vapor-deposition (CVD) growth (Wang et al. 2010; Wu et al. 2014). Due to the van der Waals interaction, the graphene coating and the dielectric core are expected to be tightly attached together.

3 Bloch mode

We now investigate the Bloch modes in graphene-coated nanowire arrays. The radius of the single nanowire is fixed at $a=40$ nm throughout the study. Under these parameters, a single graphene-coated nanowire only supports one propagating SPP mode. The effective refractive index of SPPs in single graphene-coated nanowire reaches as high as $n_{\text{eff}}\approx 20$, which indicates the modal wavelength is squeezed into a deep sub-wavelength scale. This is the result of strong field confinement of graphene SPPs.

Figure 2a shows the first Brillouin zone of the square lattice. The Bloch momentums are ($k_x=\pi$, $k_y=\pi$), ($k_x=0$, $k_y=0$), and ($k_x=\pi$, $k_y=0$) at points M, Γ, and X, respectively. We calculate the effective refractive index of the graphene-coated nanowire along the first Brillouin zone, that is, the system band structure. Figures 2b–d plot the band structure for various inter-layer spacing, while the intra-layer spacing is fixed at $d_1=320$ nm. In Fig. 2b, the intra-layer spacing is smaller than the inter-layer spacing, that is, $d_1<d_2$. One can see there are four bands supported in the system. The middle two bands are degenerated at point X and also in the range of point Γ to point M. However, the other two bands are isolated. The total bands can be regarded to be gapped. In Fig. 2b, the intra-layer spacing is equal to the inter-layer spacing, that is, $d_1=d_2$. At this critical point, the four energy bands simultaneously touch at point M. Moreover, the upper two bands the degenerate at point X. The same happens for the lower two bands. In this situation, the bandgap is closed. When the inter-layer spacing is further modified to $d_1>d_2$, the bandgap reopens as plotted

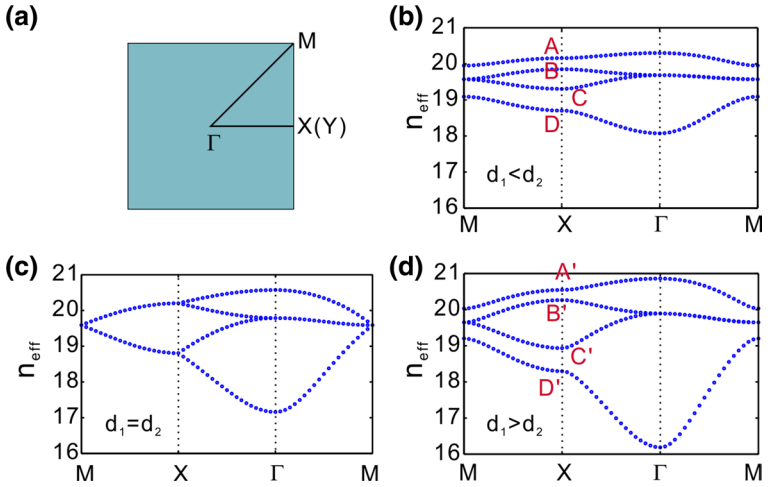

Fig. 2 Band structure of periodic two-dimensional array for different spacing. **a** First BZ of the square lattice. **b–d** Band structure for **a** $d_1=320$ nm, $d_2=400$ nm, **b** $d_1=d_2=320$ nm, and **c** $d_1=320$ nm, $d_2=280$ nm. The letters A–D and A'–D' labels the position of band structure at points X. The corresponding field distributions are present in Fig. 3

in Fig. 2d. The band structures are very similar to that in Fig. 2b. The general topological band theory states that the system experiences band inversions and topological phase of matter changes when a bandgap closes and then reopens when the system is further modified (Lu et al. 2014). Therefore, our system undergoes phase transition when $d_1=d_2$. The system is topological topological trivial for $d_1<d_2$ and non-trivial for $d_1>d_2$. The condition is the same as that in one-dimensional SSH model (Liu and Wakabayashi 2017).

The band inversion can be clearly reflected from the field distributions of Bloch modes. Figure 3 displays the field distributions at point X, that is, when Bloch momentum is $k_x=\pi$ and $k_y=0$. The electric field along propagation direction z is utilized. The letters A to D and

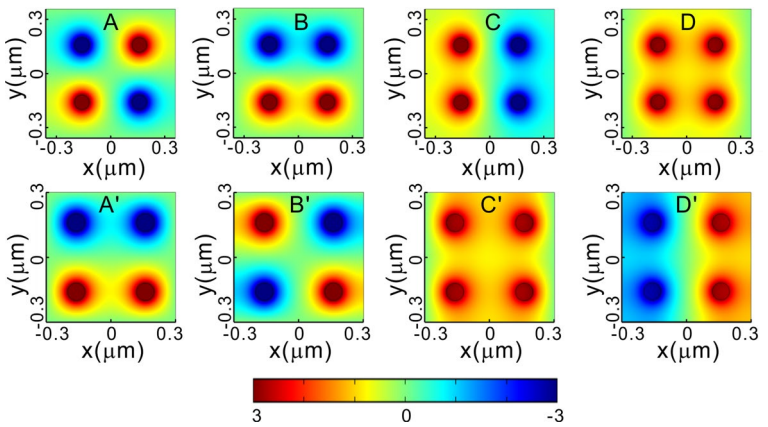

Fig. 3 Field distribution (E_z) for the Bloch modes corresponding to Fig. 2

A' to D' represent the correspondence to band structure labeled in Fig. 2b, d. A to D are for $d_1 < d_2$ and A' to D' are for $d_1 > d_2$. Despite of a phase difference of π, the field distribution of A is similar to that of B'. The fields in upper two nanowires are anti-symmetric, one is positive and the other is negative. At the same time, the field distributions along y direction are anti-symmetric as well. The field distribution of B is similar to that of A'. The fields are symmetric along x direction and anti-symmetric along y direction. The fields in upper two nanowires are negative and the lower are positive. This indicates the upper two band structures experience a band inversion when d_1 and d_2 changes their relative values. The field distribution of C and D' are also similar to each other except a phase difference. The fields along x direction are anti-symmetric and along y direction are symmetric. The field distributions of D and C' are similar to each other. The fields are symmetric along x and y directions at the same time. All the nanowires have positive fields. This indicates the lower two band structures undergo band inversion when d_1 and d_2 changes their relative values.

4 Topological edge modes

We now investigate the topological edge modes in the two-dimensional graphene-coated nanowire arrays. We consider the array is periodic in y direction and limited along x direction. The number of unit cell along x direction is N = 10. The loss of graphene is considered in the calculation.

Figure 4 plots the effective refractive index of eigenmodes in the limited systems as Bloch momentum in y direction is $k_y = 0$. In Fig. 4a, b, the inter-layer spacing is smaller than the intra-layer spacing, that is, $d_1 < d_2$. In this situation, the system is topological trivial and does not support edge modes. One can see the spectrum of effective refractive index possesses two gaps. There are no modes locating in the two gaps. Therefore, the structure does not support topological edge modes as $d_1 < d_2$. In Fig. 4c, d, the inter-layer spacing is larger than the intra-layer spacing, that is, $d_1 > d_2$. Now the system is topological non-trivial

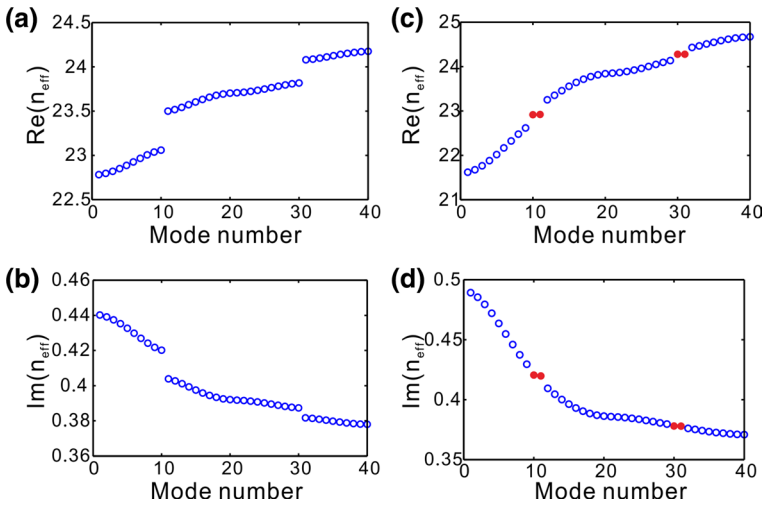

Fig. 4 Eigenvalue spectra as x direction is limited. **a**, **b** Real and imaginary parts of refractive index when $d_1 = 320$ nm and $d_2 = 400$ nm, respectively. **c**, **d** Real and imaginary parts of refractive index when $d_1 = 320$ nm and $d_2 = 280$ nm, respectively. The Bloch momentum along y direction is $k_y = 0$

and supports topological edge modes. It is noticed that there are four types of atoms in the edges; thus, there should be four edge states totally. The spectrum of effective refractive index possesses two band gaps. Each gap possesses two degenerate topological edge modes, which are marked with red color. The effective refractive index of lower and upper two edge modes is $\mathrm{Re}(n_{\mathrm{eff}})=22.93$ and 24.29, respectively. The imaginary part of refractive index of topological edge modes are $\mathrm{Im}(n_{\mathrm{eff}})=0.378$ and 0.42. The propagation distance relates to imaginary part of effective refractive index as $L_z=[2\mathrm{Im}(n_{\mathrm{eff}})k_0]^{-1}$. Therefore, the propagation distance of topological modes is $L_z=2.53$ μm and 2.27 μm, respectively.

Figure 5 shows the field distributions of four topological edge modes. The energy is surly confined at the two terminations of the arrays and exponentially decreases to the center. For the left termination, the field is mainly confined at the left two nanowires and vanished in the right two nanowires in each unit cell. For the right termination, the field is mainly confined at the right two nanowires and vanished in the left two nanowires. The vanishing amplitudes are the result of topological protection on the edge mode as it prevents the edge mode from merging with bulk modes under a continuous deformation of the system's parameters.

The edge modes in each gap are degenerate with same effective refractive index but can be distinguished through the field distributions. The field distributions of four edge modes are different. They are symmetric or anti-symmetric along x or y directions. In Fig. 5a, the fields at the left two nanowires are with same polarity but they are different from that in the right termination. The field at the left is negative while the right is positive. In Fig. 5b, the four waveguides at the two terminations of the array have same polarity. The fields in the four sites are positive. In Fig. 5c, d, the fields in two waveguides at each termination are with different polarity, one is positive and the other is negative. In Fig. 5c, the fields at two terminations are different. In Fig. 5d, the fields at two terminations are the same.

The topological edge modes are robust to topological disorders, which are determined by the difference between interlayer and intra-layer spacing d_1-d_2 (Ge et al. 2017). The edge modes persist with perturbations, such as the waveguide spacing, the refractive index

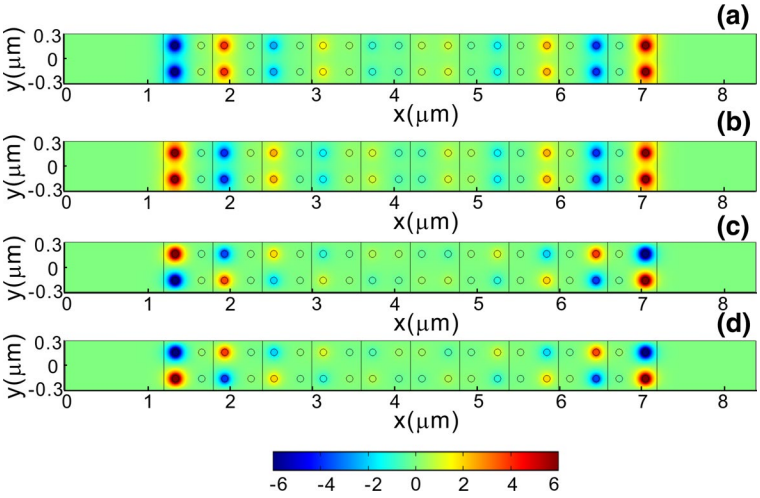

Fig. 5 Field distributions (E_z) of topological edge modes corresponding to Fig. 4b. **a**, **b** Lower two edge modes with $n_{\mathrm{eff}}=22.93$. **c**, **d** Upper two modes with $n_{\mathrm{eff}}=24.29$

of dielectric core, and the chemical potential of graphene. As shown in Fig. 6a, b, we calculate the spectra of the system as the spacing is randomly changed. The topological edge modes is robust against the slight disturbance when the perturbation of spacing is smaller than $\delta = |d_2 - d_1|$. The spacing for different unit cell is $d_1 = 314.1$ nm, 332.8 nm, 300.6 nm, 301.7 nm, 306.8 nm, 326.0 nm, 329.3 nm, 325.9 nm, 318.03 nm, 321.8 nm and $d_2 = 285.9$ nm, 267.2 nm, 299.4 nm, 298.3 nm, 293.2 nm, 274.0 nm, 270.7 nm, 274.1 nm, 282.0 nm, 278.2 nm. The results show that the four topological edge modes can still persist at the bandgap of the eigenvalues spectra. Figure 2c present the field distributions corresponding to four topological edges modes. The energy is mainly confined at the two termination of the structure, which indicates the robustness of the edge modes.

5 Conclusion

In conclusion, we have studied the topological edge modes in a two-dimensional plasmonic waveguide array. The array is composed of graphene-coated nanowire arrays and arranged in a square lattice. We show the band inversion and topological phase transition take place when the intra-layer spacing is equal to the inter-layer spacing. The transition condition is similar to that in one-dimensional SSH model. The system shows non-trivial topological property when intra-layer spacing exceeds the inter-layer spacing. The non-trivial structures support four topological edge modes and they are doubly degenerated, which can be distinguished from their field distributions. Due to the strong confinement of graphene SPPs, the modal wavelength of topological edge mode can reach as small as 1/20 of

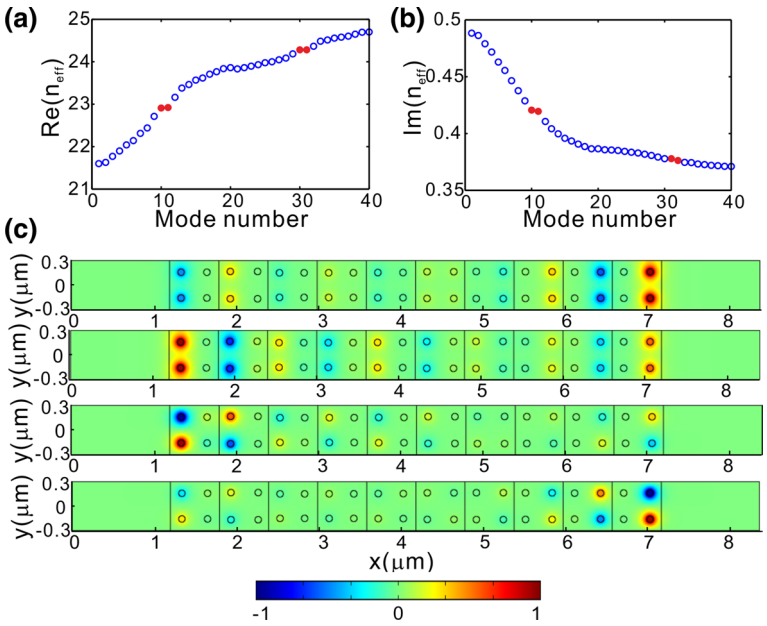

Fig. 6 The robustness of topological edge modes against disturbance of spacing. **a**, **b** Real part and imaginary part of refractive index. **c** The field distributions of topological edge modes

incident wavelength. Our results may enrich the study of SSH model and may find applications for robust light propagation at the nanoscale.

Acknowledgements This work is supported by the 973 Program (No. 2014CB921301), the National Natural Science Foundation of China (No. 11674117), Natural Science Foundation of Hubei Province (2015CFA040, 2016CFB515).

References

Bao, Q., Loh, K.P.: Graphene photonics, plasmonics, and broadband optoelectronic devices. ACS Nano **6**(5), 3677–3694 (2012)

Blanco-Redondo, A., Andrea, I., Collins, M.J., Harari, G., Lumer, Y., Rechtsman, M.C., Eggleton, B.J., Segev, M.: Topological optical waveguiding in silicon and the transition between topological and trivial defect states. Phys. Rev. Lett. **116**(16), 163901 (2016)

Chen, J., Wang, K., Long, H., Han, X., Hu, H., Liu, W., Wang, B., Lu, P.: Tungsten disulfide–gold nanohole hybrid metasurfaces for nonlinear metalenses in the visible region. Nano Lett. **18**(2), 1344–1350 (2018)

Cheng, Q., Pan, Y., Wang, Q., Li, T., Zhu, S.: Topologically protected interface mode in plasmonic waveguide arrays. Laser Photon. Rev. **9**(4), 392–398 (2015)

Deng, H., Ye, F., Malomed, B.A., Chen, X., Panoiu, N.C.: Optically and electrically tunable Dirac points and Zitterbewegung in graphene-based photonic superlattices. Phys. Rev. B **91**(20), 201402 (2015a)

Deng, H., Chen, X., Malomed, B.A., Panoiu, N.C., Ye, F.: Transverse Anderson localization of light near Dirac points of photonic nanostructures. Sci. Rep. **5**, 15585 (2015b)

Deng, H., Chen, X., Malomed, B.A., Panoiu, N.C., Ye, F.: Tunability and robustness of Dirac points of photonic nanostructures. IEEE J. Sel. Top. Quantum Electron. **22**, 5000509 (2016a)

Deng, H., Chen, X., Panoiu, N.C., Ye, F.: Topological surface plasmons in superlattices with changing sign of the average permittivity. Opt. Letters **41**(18), 4281–4284 (2016b)

Deng, H., Chen, Y., Panoiu, N.C., Malomed, B.A., Ye, F.: Surface modes in plasmonic Bragg fibers with negative average permittivity. Opt. Express **26**(3), 2559–2568 (2018)

Ge, L., Wang, L., Xiao, M., Wen, W., Chan, C.T., Han, D.: Topological edge modes in multilayer graphene systems. Opt. Express **23**(17), 21585–21595 (2015)

Ge, L., Liu, L., Xiao, M., Du, G., Shi, L., Han, D., Chan, C.T., Zi, J.: Topological phase transition and interface states in hybrid plasmonic-photonic systems. J. Opt. **19**(6), 1–5 (2017)

He, Y., He, L., Lan, P., Wang, B., Li, L., Zhu, X., Cao, W., Lu, P.: Molecular rotation movie filmed with high-harmonic generation. arXiv:1902.05662 (2019)

Hong, Z., Rezvani, S.A., Zhang, Q., Lu, P.: Octave-spanning energy-scalable CEP-stabilized pulses from a dual-chirped noncollinear optical parametric amplifier. Opt. Quantum Electron. (2017). https://doi.org/10.1007/s11082-017-1209-y

Hong, Z., Zhang, Q., Rezvani, S.: Tunable few-cycle pulses from a dual-chirped optical parametric amplifier pumped by broadband laser. Opt. Laser Technol. **98**, 169–177 (2018)

Huang, H., Ke, S., Wang, B., Long, H., Wang, K., Lu, P.: Numerical study on plasmonic absorption enhancement by a rippled graphene sheet. J. Lightwave Technol. **35**(2), 320–324 (2017)

Ke, S., Wang, B., Qin, C., Long, H., Wang, K., Lu, P.: Exceptional points and asymmetric mode switching in plasmonic waveguides. J. Lightwave Technol. **34**(22), 5258–5262 (2016)

Ke, S., Wang, B., Long, H., Wang, K., Lu, P.: Topological mode switching in a graphene doublet with exceptional points. Opt. Quantum Electron. **49**(224), 1–12 (2017a)

Ke, S., Wang, B., Long, H., Wang, K., Lu, P.: Topological edge modes in non-Hermitian plasmonic waveguide arrays. Opt. Express **25**(10), 11132–11143 (2017b)

Ke, S., Zhao, D., Liu, Q., Wu, S., Wang, B., Lu, P.: Optical imaginary directional couplers. J. Lightwave Technol. **36**(12), 2510–2516 (2018a)

Ke, S., Liu, J., Liu, Q., Zhao, D., Liu, W.: Strong absorption near exceptional points in plasmonic waveguide arrays. Opt. Quantum Electron. **50**, 318 (2018b)

Ke, S., Zhao, D., Liu, Q., Liu, W.: Adiabatic transfer of surface plasmons in non-Hermitian graphene waveguides. Opt. Quantum Electron. **50**, 393 (2018c)

Ke, S., Zhao, D., Liu, J., Liu, Q., Liao, Q., Wang, B., Lu, P.: Topological bound modes in anti-PT-symmetric optical waveguide arrays. Opt. Express **27**(10), 13858 (2019)

Kou, Y., Förstner, J.: Discrete plasmonic solitons in graphene-coated nanowire arrays. Opt. Express **24**(5), 4714–4721 (2016)
Kou, Y., Ye, F., Chen, X.: Multiband vector plasmonic lattice solitons. Opt. Lett. **38**(8), 1271–1273 (2013)
Li, M., Xie, H., Cao, W., Luo, S., Tan, J., Feng, Y., Du, B., Zhang, W., Li, Y., Zhang, Q., Lan, P., Zhou, Y., Lu, P.: Photoelectron holographic interferometry to probe the longitudinal momentum offset at the tunnel exit. arXiv:1904.09556 (2019a)
Li, L., Lan, P., Zhu, X., Huang, T., Zhang, Q., Lein, M., Lu, P.: Reciprocalspace-trajectory perspective on high harmonic generation in solids. arXiv:1809.08109 (2019b)
Li, T., Luo, L., Hupalo, M., Zhang, J., Tringides, M.C., Schmalian, J., Wang, J.: Femtosecond population inversion and stimulated emission of dense Dirac fermions in graphene. Phys. Rev. Lett. **108**(16), 167401 (2012)
Lin, X., Li, R., Gao, F., Li, E., Zhang, X., Zhang, B., Chen, H.: Loss induced amplification of graphene plasmons. Opt. Lett. **41**(4), 681–684 (2016a)
Lin, X., Rivera, N., López, J.J., Kaminer, I., Chen, H., Soljačić, M.: Tailoring the energy distribution and loss of 2D plasmons. New J. Phys. **18**(10), 105007 (2016b)
Liu, F., Wakabayashi, K.: Novel topological phase with a zero Berry curvature. Phys. Rev. Lett. **118**, 076803 (2017)
Liu, W., Wang, B., Ke, S., Qin, C., Long, H., Wang, K., Lu, P.: Enhanced plasmonic nanofocusing of terahertz waves in tapered graphene multilayers. Opt. Express **24**(13), 14765–14780 (2016)
Liu, W., Li, X., Song, Y., Zhang, C., Han, X., Long, H., Wang, B., Wang, K., Lu, P.: Cooperative enhancement of two-photon-absorption-induced photoluminescence from a 2D perovskite-microsphere hybrid dielectric structure. Adv. Funct. Mater. **28**(26), 1707550 (2018a)
Liu, Q., Ke, S., Liu, W.: Mode conversion and absorption in an optical waveguide under cascaded complex modulations. Opt. Quantum Electron. **50**, 356 (2018b)
Liu, Y., Tan, J., He, M., Xie, H., Qin, Y., Zhao, Y., Li, M., Zhou, Y., Lu, P.: Photoelectron holographic interferences from multiple returning in strong-field tunneling ionization. Opt. Quantum Electron. **51**(5):145 (2019). https://doi.org/10.1007/s11082-019-1868-y
Lu, L., Joannopoulos, J.D., Soljačić, M.: Topological photonics. Nat. Photon. **8**(11), 821–829 (2014)
Ni, G.X., Wang, L., Goldflam, M.D., Wagner, M., Fe, Z., McLeo, A.S., Liu, M.K., Keilman, F., Özyilmaz, B., Castro Neto, A.H., Hone, J., Fogler, M.M., Basov, D.N.: Ultrafast optical switching of infrared plasmon polaritons in high-mobility graphene. Nat. Photon. **10**, 244–247 (2016)
Peng, L., Zhang, L., Yuan, J., Chen, C., Bao, Q., Qiu, C.W., Peng, Z., Zhang, K.: Gold nanoparticle mediated graphene plasmon for broadband enhanced infrared spectroscopy. Nanotechnology **28**(26), 264001 (2017)
Pocock, S.R., Xiao, X., Huidobro, P.A., Giannini, V.: Topological plasmonic chain with retardation and radiative effects. ACS Photon. **5**(6), 2271–2279 (2018)
Qin, C., Zhou, F., Peng, Y., Sounas, D., Zhu, X., Wang, B., Dong, J., Zhang, X., Alù, A., Lu, P.: Spectrum Control through Discrete Frequency Diffraction in the Presence of Photonic Gauge Potentials. Phys. Rev. Lett. **120**(13), 133901 (2018). https://doi.org/10.1103/PhysRevLett.120.133901
Sun, C., Rong, K., Wang, Y., Li, H., Gong, Q., Chen, J.: Plasmonic ridge waveguides with deep-subwavelength outside-field confinements. Nanotechnology **27**, 065501 (2016)
Wang, R., Hao, Y., Wang, Z., Gong, H., Thong, J.T.L.: Large-diameter graphene nanotubes synthesized using Ni nanowire templates. Nano Lett. **10**(12), 4844–4850 (2010)
Wang, F., Qin, C.Z., Wang, B., Long, H., Wang, K., Lu, P.X.: Rabi oscillations of plasmonic supermodes in graphene multilayer arrays. IEEE J. Sel. Top. Quantum **23**(1), 4600105 (2017a)
Wang, Z., Wang, B., Long, H., Wang, K., Lu, P.: Surface plasmonic lattice solitons in semi-infinite graphene sheet arrays. J. Lightwave Technol. **35**(14), 2960–2965 (2017b)
Wang, S., Wang, B., Qin, C., Wang, K., Long, H.: Rabi oscillations of optical modes in a waveguide with dynamic modulation. Opt. Quant. Electron. (2017c). https://doi.org/10.1007/s11082-017-1220-3
Wang, F., Ke, S., Qin, C., Wang, B., Long, H., Wang, K., Lu, P.: Topological interface modes in graphene multilayer arrays. Opt. Laser Technol. **103**, 272–278 (2018)
Wu, Y., Yao, B., Zhang, A., Rao, Y., Wang, Z., Cheng, Y., Gong, Y., Zhang, W., Chen, Y., Chiang, K.S.: Graphene-coated microfiber Bragg grating for high-sensitivitygas sensing. Opt. Lett. **39**(5), 1235–1237 (2014)
Zhang, L., Zhang, Z., Kang, C., Cheng, B., Chen, L., Yang, X., Wang, J., Li, W., Wang, B.: Tunable bulk polaritons of graphene-based hyperbolic metamaterials. Opt. Express **22**(11), 14022–14030 (2014)
Zhao, D., Wang, Z., Long, H., Wang, K., Wang, B., Lu, P.: Optical bistability in defective photonic multilayers doped by graphene. Opt. Quantum Electron. **49**, 163 (2017)

Zhao, D., Liu, W., Ke, S., Liu, Q.: Large lateral shift in complex dielectric multilayers with nearly parity–time symmetry. Opt. Quant. Electron. (2018). https://doi.org/10.1007/s11082-018-1593-y
Zhao, D., Zhong, D., Hu, Y., Ke, S., Liu, W.: Imaginary modulation inducing giant spatial Goos–Hänchen shifts in one-dimensional defective photonic lattices. Opt. Quantum Electron. **51**, 113 (2019)

Publisher's Note Springer Nature remains neutral with regard to jurisdictional claims in published maps and institutional affiliations.